Signal Processing 89 (2009) 1162–1175

Contents lists available at ScienceDirect

Signal Processing

journal homepage: www.elsevier.com/locate/sigpro

Multirate adaptive filtering for low complexity DS/CDMA code acquisition

Hua-Lung Yang *, Wen-Rong Wu

Department of Communication Engineering, National Chiao-Tung University, Hsin Chu 300, Taiwan, ROC

ARTICLE INFO

Article history:
Received 1 June 2008
Received in revised form
27 October 2008
Accepted 27 December 2008
Available online 10 January 2009

Keywords:
Code acquisition
Low complexity
Adaptive filtering
Multirate signal processing
DS/CDMA

ABSTRACT

Code acquisition in CDMA systems is conventionally conducted with a matched-filter based structure. However, the performance of this method degrades greatly while multiple access interference presents. Recently, an adaptive filtering scheme was proposed to solve this problem. It has been shown that the computational complexity of this approach is proportional to the delay uncertainty and inversely proportional to the required acquisition time. When propagation delay is large and the required acquisition time is short, the computational complexity of the adaptive filtering approach will become high. In this paper, we propose a multirate adaptive code acquisition approach to alleviate this problem. The proposed scheme is comprised of several acquisition units operating in different processing rates. Thanks to the decimation property in multirate processing, the overall computational complexity can be greatly reduced. Theoretical analysis of adaptive filters and mean acquisition time is also provided. Experimental results show that while the proposed scheme can have comparable performance with respect to the original adaptive acquisition scheme, its computational complexity is much lower.

1. Introduction

Code-division multiple access (CDMA) is a promising technique for wireless mobile communication. It is well known that the main performance bottleneck for a CDMA system is the multiple access interference (MAI). MAI not only affects detection, but also code synchronization. Code synchronization can be further divided into code acquisition and code tracking. In this paper, we consider code acquisition with MAI. Code acquisition has been widely studied in the literature. The conventional approach to this problem is the well-known matched-filter (MF) based method [1–10,32,36] (and references therein). The MF can have a serial [1], parallel [2–4], or hybrid search structure providing an easy trade-off between hardware complexity and acquisition time. However, the MF-based method is only optimal for the single-user case. The acquisition performance degrades greatly when MAI presents, especially in near–far environments [5,6]. To evaluate the performance of an acquisition scheme, a measure called acquisition-based capacity was defined in [7]. This capacity corresponds to the maximum number of users that a system can serve (with certain acquisition performance). It was shown in [7,19] that the asymptotic acquisition-based capacity for the MF is $L/[2\ln(L)]$, where L is the processing gain. The quantity is less than the bit-error-rate-based capacity [8] which is proportional to L. This implies that code acquisition may become a limiting factor for a CDMA system capacity. Another discussion on the acquisition-based capacity for the MF can be found in [9].

Another category of the acquisition technique qemploys subspace- or matrix-based methods [11–18]. The

* Corresponding author. Tel.: +886 35 731647.
E-mail addresses: hlyang28@gmail.com, aquariuscottt@gmail.com (H.-L. Yang), wrwu@faculty.nctu.edu.tw (W.-R. Wu).

0165-1684/$ - see front matter © 2009 Elsevier B.V. All rights reserved.
doi:10.1016/j.sigpro.2008.12.024

advantage of subspace-based approaches is that it does not require training sequences. However, these methods usually have to estimate, decompose, and inverse the autocorrelation matrix of the received signal vector. This often demands high computational complexity, especially at a large processing gain. The projection degree measurement (PDM) algorithm [11] observes two successive symbols in order to obtain the complete information of one desired symbol. As a consequence, the PDM has to estimate and inverse an autocorrelationmatrix of dimension $2L$-by-$2L$. The multiple signal classification (MUSIC) algorithm has also been applied to code acquisition [12–14]. The MUSIC algorithm has to carry out eigen-decompositions and extract eigen-vectors corresponding to noise subspace. Despite of the oversampling operation in [12], the computational complexity of the MUSIC algorithm is with $\mathcal{O}(L^3)$. Besides, this algorithm is constrained under $2K<L$, where K is the number of users. A matrix-based method [18] called a large sample maximum likelihood (LSML) acquisition algorithm, provides excellent performance and robustness against the near-far problem. However, it requires a large amount of received bit signals and, again, pays a high computational complexity in the matrix operations. Notably, these methods are specifically designed for CDMA systems with periodic spreading codes (i.e., the spreading code repeats itself for every bit) and may not straightforwardly apply to the aperiodic-code systems (i.e., the periodicity of the spreading code is great than a bit interval).

Recently, the adaptive filter technique [19–26] was proposed to solve the acquisition problem in the presence of MAI. The method [19–24] separates the delay uncertainty into several regions, named (delay) cells. The input to the adaptive filter is the desired user's pseudo-noise (PN) sequence with a code delay associated to a cell. Each cell is then sequentially tested and the code delay can then be estimated with the location of the maximum convergent tap-weight. This method can also have a serial or parallel searching structure trading performance with computational complexity. It was addressed in [19,20] that the adaptive filtering scheme can have a much higher acquisition-based capacity than the MF. Apart from the maximum weight testing, architectures with the threshold testing were also considered [21,22]. The threshold can be set for the mean-squared error (MSE) or for the maximum tap-weight (in a cell). It was found in [23] that the tap-weight testing can bring better performance than the MSE testing. The acquisition performance with fading channels was analyzed and reported in [24]. Yet, another adaptive receiver structure reported in [26] performs an exhaustive search to find the integer chip delay, and then solve aquadratic equation to find the corresponding fractional chip delay. The drawback of this approach is that its complexity is high particularly for a large processing gain.

In this paper, we propose a code acquisition algorithm using a multirate adaptive filtering technique. Similar to the original adaptive filter approach [19,20], our structure is valid for periodic as well as for aperiodic spreading codes. In fact, many commercial CDMA systems, including IS-95 standard [28], CDMA-2000 proposal [29], and 3G CDMA-based wireless networks [30,31], adopt aperiodic codes for spreading. The fundamental structure of the proposed algorithm is similar to that in [19,20]; however, the proposed scheme contains several adaptive filters operating in different rates. The adaptive filters with low rates will search the code delay in low resolutions. The adaptive filters with higher rates will then resolve the code delay in higher resolutions. The adaptive filter with the highest rate, say the chip-rate, can finally identify the original code delay. The proposed multirate processing can have a much lower computational complexity than the conventional adaptive filtering approaches in [19,20]. This is particularly true in the applications where the processing gain as well as the delay uncertainty is large.

Throughout this paper, the notations $(\cdot)^{\mathrm{T}}$ and $\mathbf{A}_{u,v}$ denote the transposition operator and the uvth entry of a matrix $\mathbf{A}$, respectively. Also, $\lceil y \rceil$ indicates the smallest integer greater than or equal to the value y, whereas $\lfloor y \rfloor$ the largest integer smaller than or equal to y. Besides, z represents the unit delay operator, $\mathbf{I}$ the identity matrix, and $E\{\cdot\}$ the statistical expectation operation. The rest of this paper is organized as follows. Section 3 reviews the conventional adaptive code acquisition scheme. Section 3 describes the proposed multirate code acquisition scheme. Section 4 analyzes the performance of the proposed scheme, and Section 5 reports simulation results. Finally, we draw conclusions in Section 6.

2. Conventional adaptive code acquisition

In this section, we briefly review the conventional adaptive code acquisition scheme [19,20]. Fig. 1 shows the structure of this scheme. For reference convenience, we name this scheme as a one-rate (1R) scheme since only one processing rate (i.e., chip-rate) is used. The baseband chip-rate sampled received signal can be expressed as

$$r(n)=\sum_{k=1}^{K}A_k x_k(n-\tau_k)+w(n), \tag{1}$$

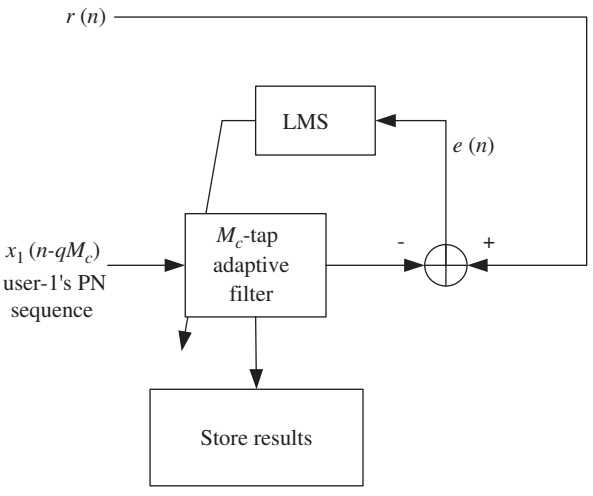

Fig. 1. Conventional 1R code acquisition system, where $x_1(n-qM_c)$ is user-1's PN sequence at qth cell with $q=0,\ldots,Q-1$.

where K, τ_k, A_k, $x_k(n)$, and $w(n)$ denotes the number of user, the code delay, the signal amplitude, the transmitted signal of user-k, and channel noise, respectively. The channel noise is assumed to be additive white Gaussian and its mean is zero. The transmitted signal of user-k can be expressed as

$$x_k(n)=\sum_{j=-\infty}^{\infty} d_k(j)\sum_{l=0}^{L-1} c_{kj}(l)p(n-l-jL),\quad k=1,\ldots,K, \tag{2}$$

where $d_k(j)$ denotes the jth BPSK signal of user-k and $c_{kj}(l)\in\{1,-1\}$ corresponds to the lth chip signal in $d_k(j)$. Also, L denotes the processing gain and $p(n)$ the chip-rate sampled pulse. Before proceed further, we list assumptions to be used in the sequel:

(a) User-1's code delay is of interest and $A_1=1$.
(b) The code delay is an integer multiples of the chip-duration and smaller than L.
(c) Carrier synchronization is established before code acquisition.
(d) No data are modulated for user-1's signal in the period of code acquisition, i.e., $d_1(j)=1$.
(e) The chip-pulse is considered as a rectangular pulse with unit amplitude.
(f) The code sequence $c_{k,j}$ has a period much higher than the processing gain such that the input to the adaptive filter can be viewed as statistically white.
(g) Only the additive white Gaussian noise (AWGN) channel is considered and the summation of MAI and white Gaussian noise can be modeled as another white Gaussian noise [32].

The 1R scheme first divides L into $Q=\lceil L/M_c\rceil$ cells, where M_c is the length of the adaptive filter. The adaptive filter then serially searches the code delay in these cells. The least-mean-square (LMS) algorithm is employed to minimize the MSE between the received signal $r(n)$ and the adaptive filter output (see Fig. 1). The tap-weight update equations are given by

$$\mathbf{w}^q(n+1)=\mathbf{w}^q(n)+\mu_c e(n)\mathbf{x}^q(n), \tag{3}$$

$$e(n)=r(n)-[\mathbf{w}^q(n)]^{\mathrm{T}}\mathbf{x}^q(n),\quad q\in\{0,\ldots,Q-1\}, \tag{4}$$

where μ_c denotes the step size controlling the convergence of the adaptive filter, $\mathbf{w}^q(n)=[w_0^q(n),w_1^q(n),\ldots,w_{M_c-1}^q(n)]^{\mathrm{T}}$ the filter tap-weight vector for the qth cell, and $\mathbf{x}^q(n)=[x_1(n-qM_c),x_1(n-qM_c-1),\ldots,x_1(n-qM_c-M_c+1)]^{\mathrm{T}}$ the corresponding input vector. Here, q is sequentially increased from zero to $Q-1$. The tap-weight vector $\mathbf{w}^q(n)$ for a particular q is stored after some iterations, say N_1 chips. Then, an estimation of τ_1 can be derived with the tap-index of the maximum tap-weight (among all cells). Let the $\hat{\Delta}_c$th tap ($0\leqslant\hat{\Delta}_c<M_c$) of the adaptive filter in the $\hat{\alpha}_c$th cell has the maximum value. Then, we can have the delay estimation $\hat{\tau}_1=\hat{\alpha}_cM_c+\hat{\Delta}_c$. Combine $\mathbf{w}^q(N_1)$, $q=0,1,\ldots,Q-1$ into a big vector $\mathbf{w}$, i.e., $\mathbf{w}=[[\mathbf{w}^0(N_1)]^{\mathrm{T}},[\mathbf{w}^1(N_1)]^{\mathrm{T}},\ldots,[\mathbf{w}^{Q-1}(N_1)]^{\mathrm{T}}]^{\mathrm{T}}$. It can be shown that the probability of acquisition error is

$$P_e=1-P_b(w_c\geqslant w_j),\quad c\neq j,\quad \{c,j\}\in\{0,1,\ldots,L-1\}, \tag{5}$$

where w_j denotes the jth element of $\mathbf{w}$ and w_c the tap-weight corresponding to the true code delay τ_1 (i.e., $c=\tau_1$). To evaluate (5), we need to know the stochastic properties of the tap-weights. It has been shown in [33] that these tap-weights at convergence have Gaussian distributions with a mean vector of

$$\mathbf{m}_{(L\times1)}=\mathbf{w}_o, \tag{6}$$

and a covariance matrix of

$$\mathbf{C}_{(L\times L)}\approx\frac{\mu_c}{2}J_{min}\mathbf{I} \tag{7}$$

$$\triangleq\sigma_w^2\mathbf{I}, \tag{8}$$

where $\mathbf{w}_o$ is the optimum solution of $\mathbf{w}$ solved with the Wiener equations [34], J_{min} is the corresponding minimum mean-squared error (MMSE), and σ_w^2 is the variance of each tap-weight. Let $\mathbf{R}^q=E\{\mathbf{x}^q(n)[\mathbf{x}^q(n)]^{\mathrm{T}}\}$ and $\mathbf{p}^q=E\{\mathbf{x}^q(n)r(n)\}$. Since the input is white, $\mathbf{R}^q=\mathbf{I}_{M_c\times M_c}$. It is well known that $\mathbf{w}_o^q=(\mathbf{R}^q)^{-1}\mathbf{p}^q$. Let $\tau_1=\alpha_cM_c+\Delta_c$, $0\leqslant\Delta_c<M_c$, and p_j^q is the jth entry of $\mathbf{p}^q$ ($j\in\{0,1,\ldots,M_c-1\}$). It is simple to show that $p_j^q=1$ when $q=\alpha_c$ and $j=\Delta_c$, and $p_j^q=0$ otherwise. This is to say that a unique peak with value one will appear in w_c, and all other weights are zeros. Thus, we can have $J_{min}=E\{r^2(n)\}-1$. Using Eqs. (6) and (8), we can rewrite (5) as

$$P_e=1-\int_{-\infty}^{\infty}\left[1-Q\left(\frac{w_c}{\sigma_w}\right)\right]^{L-1}\exp\left(-\frac{(w_c-1)^2}{2\sigma_w^2}\right)\mathrm{d}w_c, \tag{9}$$

where $Q(\cdot)$ denotes the Q-function [35]. It is known that an M_c-tap adaptive filter (with the LMS algorithm) requires $2M_c$ multiplications per iteration. Thus, the computational complexity is proportional to the filter size.

3. Proposed adaptive multirate code acquisition

To understand our idea easier, we start our development with a two-rate (2R) system. Then, we will extend it to a three-rate (3R) system.

3.1. 2R scheme

Following the assumptions given in Section 2, we express (1) as

$$\begin{aligned} r(n)&=\sum_{k=1}^{K}A_kx_k(n-\tau_k)+w(n)\\ &=x_1(n-\tau_1)+v(n), \end{aligned} \tag{10}$$

where

$$v(n)=\sum_{k=2}^{K}A_kx_k(n-\tau_k)+w(n) \tag{11}$$

denotes the sum of MAI and white Gaussian noise. Let the variance of $v(n)$ be σ_v^2. For notational simplification, we will omit the subscripts of $x_1(n)$ and τ_1 in following derivations. Fig. 2 shows the architecture of the proposed 2R acquisition system. As we can see, the system contains two units with two different processing rates. We call the unit in Fig. 2(a) as a low-rate unit (LRU). In this unit, the adaptive filter updates its tap-weights with a low rate. For

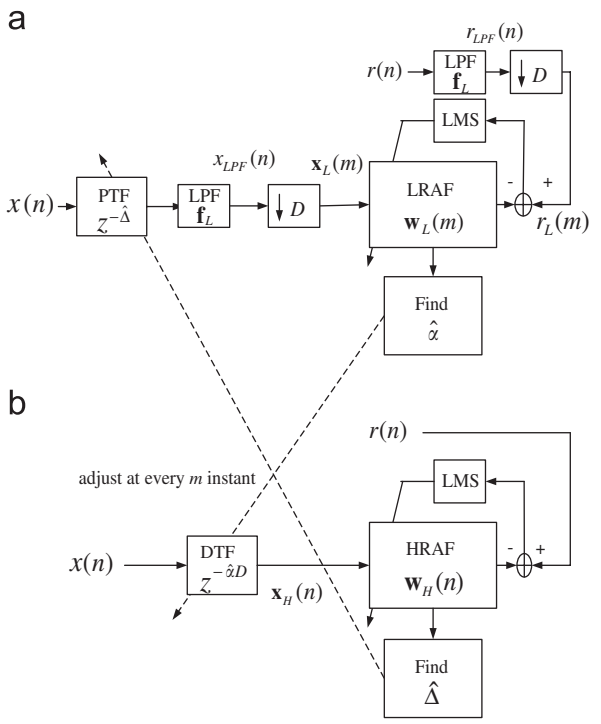

Fig. 2. Proposed 2R code acquisition system with (a) LRU and (b) HRU. Note that LRU and HRU interact only when $n = mD$. The dash-lines indicate feedforward and feedback operations.

this reason, we refer to the adaptive filter in this unit as a low-rate adaptive filter (LRAF). By contrast, we call the unit in Fig. 2(b) a high-rate unit (HRU). The adaptive filter in this unit updates its tap-weights with a high rate. We refer to the adaptive filter in this unit as a high-rate adaptive filter (HRAF). Note that the high-rate here denotes the chip-rate. There are feedforward and feedback operations in the system. We now describe the fundamental feedforward operation. First, consider Fig. 2(a). The system passes the received signal $r(n)$ and the locally generated user-1's signal $x(n)$ through lowpass filters (LPFs) to obtain $r_{LPF}(n)$ and $x_{LPF}(n)$, respectively. Then, it downsamples these signals with a factor of D and feeds the resultant signals to the LRAF. Let $M_p = \lceil L/D \rceil$. Then, the code delay can be rewritten as $\tau = \alpha D + \Delta$ where $\alpha \in \{0, 1, \ldots, M_p\}$ and $-D/2 < \Delta \leqslant D/2$. Note that the ranges of α and Δ are defined different from that in the previous section. The LRAF will adapt to estimate a low-resolution τ having the value in $\{0, D, \ldots, M_p D\}$. Similar to the 1R system, we select the tap-index associating with the maximum tap-weight value. Note that $M_p + 1$ is the filter length of the LRAF and $(M_p + 1)D$ must be great or equal to L. Let theindex with the maximum tap-weight in the LRAF be $\hat{\alpha}$. The HRU in Fig. 2(b) then delays $x(n)$ with $\hat{\alpha}D$ chips. We call the device to perform the delay function as the delay-tuning filter (DTF). With this operation, the HRAF adapts to refine the code-delay resolution. After convergence, we select the tap-index $\hat{\Delta}$ with the maximum tap-weight. It is easy to see that the index should be in the range of $\pm D/2$. Combing these two tap-weight indices, we can finally obtain a code-delay estimate. In summary, the LRU attempts to acquire τ in a multi-chip level (low resolution), while the HRU in a chip level (high resolution).

We now examine some properties of the 2R feedforward operation. For low complexity consideration, we let the LPF filtered $r(n)$ (in (10)) as

$$r_{LPF}(n) = \sum_{j=0}^{D-1} r(n-j) = \sum_{j=0}^{D-1} x(n-\tau-j) + v_{LPF}(n), \tag{12}$$

where

$$v_{LPF}(n) = \sum_{j=0}^{D-1} v(n-j). \tag{13}$$

It is simple to see that this is just an averaging operation with a D-tap filter (apart from a constant). In Fig. 2(a), $\mathbf{f}_L$ indicates a vector consisting of the impulse response of the LPF. As shown, each element of $\mathbf{f}_L$ has the value of one. Substituting $\tau = \alpha D + \Delta$, we can rewrite (12) as

$$r_{LPF}(n) = \sum_{j=0}^{D-1} x(n-\alpha D-\Delta-j) + v_{LPF}(n). \tag{14}$$

Downsampling (14) with a factor of D, we then have

$$r_L(m) \triangleq r_{LPF}(n)|_{n=mD} = \sum_{j=0}^{D-1} x((m-\alpha)D-\Delta-j) + v_L(m), \tag{15}$$

where we let $m = \lfloor n/D \rfloor$ and $v_L(m) = v_{LPF}(mD)$. Similarly, we can average $x(n)$ to obtain

$$x_{LPF}(n) = \sum_{j=0}^{D-1} x(n-j), \tag{16}$$

and downsample $x_{LPF}(n)$ to obtain

$$x_L(m) \triangleq x_{LPF}(n)|_{n=mD} = \sum_{j=0}^{D-1} x(mD-j). \tag{17}$$

Let the input vector of the LRAF be $\mathbf{x}_L(m)$. Then, we have

$$\mathbf{x}_L(m) = [x_L(m), x_L(m-1), \ldots, x_L(m-M_p)]^{\mathrm{T}}. \tag{18}$$

For a different value of Δ, the performance of the LRAF will be different. To evaluate the impact of Δ on LRAF, we calculate the optimal tap-weights and the corresponding steady-state MSE. We put the detailed derivation in Appendix A, and summarize the result below. For $\Delta \geqslant 0$, we have the optimal tap-weights as

$$w_{L,o,\varepsilon} = \begin{cases} 1-\rho, & \varepsilon = \alpha, \\ \rho, & \varepsilon = \alpha+1, \\ 0 & \text{otherwise}, \end{cases} \quad \varepsilon \in \{0, 1, \ldots, M_p\}, \tag{19}$$

and the steady-state MSE as

$$J_L(\infty) = \left[1 + \frac{(M_p+1)\mu_L}{2}\right] J_{L,min}. \tag{20}$$

For $\Delta < 0$, we have

$$w_{L,o,\varepsilon} = \begin{cases} 1-\rho, & \varepsilon = \alpha, \\ \rho, & \varepsilon = \alpha-1, \\ 0 & \text{otherwise}, \end{cases} \quad \varepsilon \in \{0, 1, \ldots, M_p\}, \tag{21}$$

and

$$J_L(\infty)=\left[1+\frac{(M_p+1)\mu_L}{2}\right]J_{L,min}, \tag{22}$$

where $\rho=|\Delta|/D$ and $J_{L,min}$ is defined in (A.14), respectively. Using (A.14) and observing $0\leqslant\rho\leqslant 1/2$, we see that when ρ gets larger, $J_{L,min}$ will become larger. This will also make the steady-state MSE in (22) larger. When $\Delta=0$, $\rho=0$ and τ can be divided by D. The response of the LRAF can be seen as a perfectly downsampled version of the channel response. If the channel has an impulse-like response, so does the LRAF. When $\Delta>0$ (or $\Delta<0$), $\tau>\alpha D$ (or $\tau<\alpha D$). In both cases, τ cannot be divided by D. The response of the LRAF cannot have an impulse-like response. From Eqs. (A.12) and (A.37), we see that a nonzero ρ ($\Delta=0$) will produce two nonzero weights and make the value of the peak tap-weight smaller than one. Combining these effects, we can conclude that the larger the ρ, the worse the acquisition performance. The worst case occurs when $\rho=1/2$ yielding two nonzero equal weights. In what follows, we will develop a system that can null ρ.

Now, let us consider operations in the HRU. As Fig. 2(b) shows, the input to the HRAF is $x(n-\hat{\alpha}D)$. As mentioned, the optimal filter of the LRAF may have two nonzero weights with the same value. Thus, the peak position can be α or $\alpha+1$. In other words, we need at least $D+1$ taps for the HRAF. To simplify our analysis, we let $\hat{\alpha}=\alpha$. It is simple to see that the optimal weights of the HRAF will have a unique peak at $\hat{\Delta}$. Since the analysis of HRAF is straightforward, we only provide the results without detailed derivations. Let

$$\begin{aligned}\mathbf{x}_H(n)&=[x(n-\hat{\alpha}D+D/2),\ldots,x(n-\hat{\alpha}D),\ldots,x(n-\hat{\alpha}D-D/2)]^{\mathrm{T}}\\&\triangleq[x_{H,-D/2}(n),\ldots,x_{H,0}(n),\ldots,x_{H,D/2}(n)]^{\mathrm{T}}\end{aligned} \tag{23}$$

$$\mathbf{w}_H(n)\triangleq[w_{H,-D/2}(n),\ldots,w_{H,0}(n),\ldots,w_{H,D/2}(n)]^{\mathrm{T}}, \tag{24}$$

where we assume that $D/2$ is an integer (for notational convenience). Notice that $\mathbf{R}_H\triangleq E\{\mathbf{x}_H(n)\mathbf{x}_H^{\mathrm{T}}(n)\}=\mathbf{I}$. We then have the optimum weights listed below:

$$w_{H,oj}=\begin{cases}1, & j=\Delta,\\ 0 & \text{otherwise},\end{cases} \tag{25}$$

where $w_{H,oj}$ is the jth element of $\mathbf{w}_{H,o}$, and $\mathbf{w}_{H,o}$ is the optimal solution of $\mathbf{w}_H(n)$. We then have the MMSE and steady-state MSE as

$$\begin{aligned}J_{H,min}&=E\{[r(n)-\mathbf{w}_H^{\mathrm{T}}(n)\mathbf{x}_H(n)]^2\}|_{\mathbf{w}_H(n)=\mathbf{w}_{H,o}}\\&=E\{r^2(n)\}-2\mathbf{w}_{H,o}^{\mathrm{T}}E\{\mathbf{x}_H(n)r(n)\}+\mathbf{w}_{H,o}^{\mathrm{T}}\mathbf{R}_H\mathbf{w}_{H,o}\\&=\sigma_v^2,\end{aligned} \tag{26}$$

$$J_H(\infty)=\left[1+\frac{(D+1)\mu_H}{2}\right]J_{H,min}, \tag{27}$$

where μ_H is the step size used in the HRAF.

The main problem associated with the 2R scheme described above is that sampling phases for $r_{LPF}(n)$ and $x_{LPF}(n)$ may not be synchronized (i.e., $\Delta\neq 0$). As analyzed, the acquisition performance can be greatly affected when Δ is not equal to zero. Our remedy to this problem is to adjust the sampling phase of $x(n)$ during filter adaptation. This is possible if Δ estimated by the HRAF can be feedback to the LRAF. To realize this thought, we use a device, namely phase-tuning filter (PTF), to tune the input phase with $\hat{\Delta}$ chips (see the feedback operation in Fig. 2). The PTF can advance or lag the phase of its input signal. Practically, the PTF can be implemented with a buffer and a multiple-input-to-one-output selector. With this structure, the sampling phases for $r_{LPF}(n)$ and $x_{LPF}(n)$ can be synchronized and, therefore, (A.12) can have a unique peak. Note that the LRU and HRU interact only when $n=mD$. Letting $\Delta=0$ (i.e., $\rho=0$) in Eqs. (A.14) and (A.25), we have

$$J_{L,min}=D\sigma_v^2, \tag{28}$$

$$\mathbf{Q}_{\varepsilon,\varepsilon}(m)=\frac{\mu_L}{2}D\sigma_v^2,\quad \varepsilon\in\{0,\ldots,M_p\}. \tag{29}$$

Thus, steady-state MSEs of the LRAF and the HRAF are

$$J_L(\infty)=\left[1+\frac{(M_p+1)\mu_L}{2}\right]D\sigma_v^2, \tag{30}$$

$$J_H(\infty)=\left[1+\frac{(D+1)\mu_H}{2}\right]\sigma_v^2. \tag{31}$$

3.2. 3R scheme

In the previous subsection, we have proposed a 2R scheme that is able to null ρ. Since the HRAF operates in a high processing rate, it dominates the overall computational complexity. This becomes an important issue when the tap-length $D+1$ is large. We can solve the problem by introducing a unit with another processing rate. We call this unit as a medium-rate unit (MRU). This unit contains a medium-rate adaptive filter (MRAF) sharing the computational loading of the HRAF. As shown in Fig. 3(b), the LPFs $\mathbf{f}_M$ average $r(n)$ and $x(n)$ with a window side of D_M, and the decimators downsample the resultant signals with a factor of D_M. Let the DPTF denote the device cascading the DTF and PTF. Here, the processing rate of the MRU is D/D_M times faster than that of the LRU, but D_M times slower than that of the HRU.

With the additional MRU, we have three resolutions to work with. We can express the code delay as $\tau=\alpha D+\beta D_M+\delta$, where $\alpha\in\{0,1,\ldots,M_p\}$, $\beta\in\{-D/(2D_M),\ldots,0,\ldots,D/(2D_M)\}$, and $\delta\in\{-D_M/2,\ldots,0,\ldots,D_M/2\}$. For convenience, again, we assume that $D/(2D_M)$ and $D_M/2$ are integers. Then, we use the LRU, MRU and HRU to estimate $\{\alpha,\beta,\delta\}$, respectively. Note that $-(D+D_M)/2\leqslant\beta D_M+\delta\leqslant(D+D_M)/2$, where $D_M\geqslant 2$. In other words, the MRAF and HRAF can span a delay region greater than $D+1$. Define the tap-weight vector and the input vector of the MRAF as

$$\mathbf{w}_M(s)\triangleq[w_{M,-D/(2D_M)}(s),\ldots,w_{M,0}(s),\ldots,w_{M,D/(2D_M)}(s)]^{\mathrm{T}}, \tag{32}$$

$$\mathbf{x}_M(s)\triangleq[x_{M,-D/(2D_M)}(s),\ldots,x_{M,0}(s),\ldots,x_{M,D/(2D_M)}(s)]^{\mathrm{T}}, \tag{33}$$

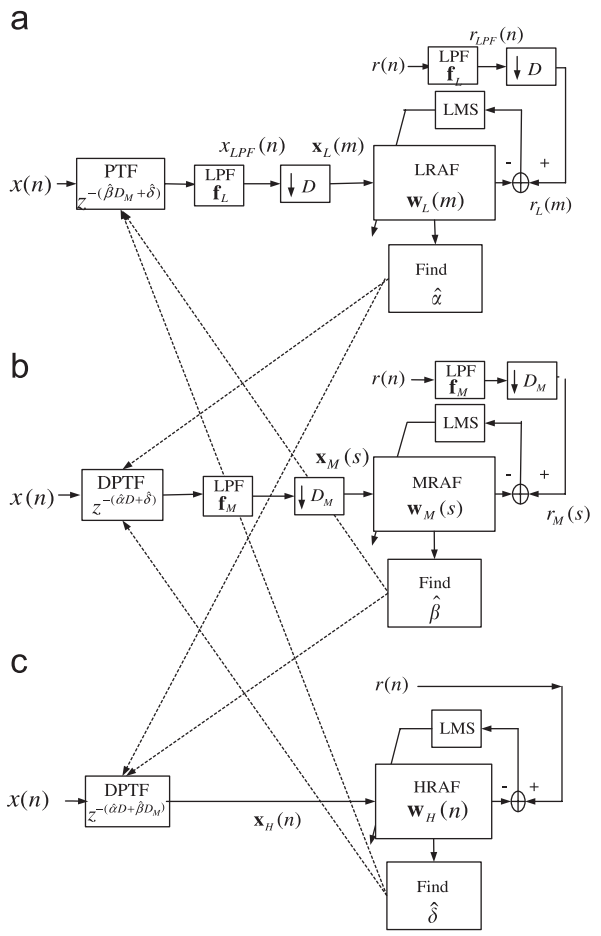

Fig. 3. Proposed 3R code acquisition system with (a) LRU, (b) MRU, and (c) HRU. Again, all units interact only when $n = mD$ and the dash-lines are for feedforward and feedback operations.

where $s = \lfloor n/D_M \rfloor$. The update equation for the MRAF is given by

$$\mathbf{w}_M(s) = \mathbf{w}_M(s-1) + \mu_M \mathbf{x}_M(s)[r_M(s) - \mathbf{x}_M^{\mathrm{T}}(s)\mathbf{w}_M(s-1)], \tag{34}$$

where μ_M is the corresponding step size and

$$r_M(s) = \sum_{j=0}^{D_M-1} r(n-j)|_{n=sD_M}, \tag{35}$$

$$x_{M,\varepsilon}(s) = \sum_{j=0}^{D_M-1} x(n - \hat{\alpha}D - \hat{\delta} - \varepsilon D_M - j)|_{n=sD_M},$$
$$\varepsilon \in \{-D/(2D_M), \ldots, 0, \ldots, D/(2D_M)\}, \tag{36}$$

where we have used $\hat{\alpha}D$ and $\hat{\delta}$ obtained from other two units. The weight adaptations for the LRAF and HRAF are similar to (A.19).

We have analyzed the performance of the HRAF and LRAF in a 2R system previously. The performance of the MRU in a 3R system can be done in a similar way. We can treat the MRU as a special LRU, and replace D with D_M for the formulas derived for the LRAF. Since this is straightforward, we omit the detailed results here. Note that in Fig. 3 all units update parameters in their PTFs or DTFs simultaneously at $n = mD$. Let the estimates for α, β, and δ at the instant $n = mD$ be $\hat{\alpha}(m)$, $\hat{\beta}(s)$, and $\hat{\delta}(n)$, respectively. When $n = mD$, the PTF in the LRU delays $x(n)$ by $\hat{\beta}(s)D_M + \hat{\delta}(n)$ chips, the DPTF in the MRU delays $x(n)$ by $\hat{\alpha}(m)D + \hat{\delta}(n)$ chips, and the DPTF in the HRU delays $x(n)$ by $\hat{\alpha}(m)D + \hat{\beta}(s)D_M$ chips. We can extend the idea to a four-rate or higher rate system; however, the system architecture will become complex. For typical applications, a 2R or 3R system will be sufficient. As described, all the filters are adjusted using the LMS algorithm. As shown later, the tap-weight of an adaptive filter can be treated as a random variable. Thus, α, β, or δ may be incorrectly estimated during the adaptation, which we call a decision error. Note that the LMS algorithm changes the filter-weight values slowly. For most cases, theestimation error can be corrected shortly. There are only few cases that the error will propagate between adaptive filters and the overall effect may lower the final amplitudes of the peak tap-weights. To alleviate the decision error problem, we can let the LRU operate for a short period of time without feedback at the initial. Simulations show that the error propagation effect only slightly slows the convergence.

4. Performance analysis

To compare the proposed schemes with the 1R system in Section 2, we employ some performance measures such as the required computational complexity (per iteration), acquisition error probability, and mean acquisition time.

4.1. Computational complexity

To have a fair comparison, we let $N = N_1 = N_M$, where N_M denotes the iteration time of the multirate system. Also, we let $D = Q$ such that the filter size in the 1R system is approximately equal to that of the LRAF ($M_c \approx M_p + 1$). Since the main operation in filtering is multiplication, we only take this into account. We first calculate the total multiplications required in N iterations and then divide the result by N.

4.1.1. 1R scheme

As mentioned in Section 2, the M_c-tap adaptive filter will require $2M_c$ multiplications per iteration. Then, the computational complexity of the 1R system, denoted as C_1, is $2M_c = 2\lceil L/D \rceil$.

4.1.2. 2R scheme

For the 2R scheme, we have to take both the LRAF and HRAF into account. Since the HRAF has $D+1$ taps and operates in the chip-rate, it requires $2(D+1)$ multiplications per iteration. On the other hand, the LRAF has $M_p + 1$ taps operating in a rate D times slower. Thus, the required multiplications per iteration for a 2R scheme, C_2,

is given by

$$C_2 = \frac{2(M_p+1)\frac{N}{D} + 2(D+1)N}{N} \tag{37}$$

$$= \frac{2(M_p+1)}{D} + 2(D+1). \tag{38}$$

4.1.3. 3R scheme

Similarly, we take the LRAF, MRAF, and HRAF into account. The required multiplication per iteration for a 3R system, C_3, turns out to be

$$C_3 = \frac{2(M_p+1)\frac{N}{D} + 2\left\lceil\frac{D+1}{D_M}\right\rceil\frac{N}{D_M} + 2(D_M+1)N}{N} \tag{39}$$

$$= \frac{2(M_p+1)}{D} + \frac{2}{D_M}\left\lceil\frac{D+1}{D_M}\right\rceil + 2(D_M+1), \tag{40}$$

where $\lceil (D+1)/D_M \rceil$ is the minimum required tap-length for the MRAF.

4.2. Probability of acquisition error

For a general LMS adaptive filter with a step size μ_c, the time to converge can be evaluated using $\lceil 1/\mu_c \rceil$ (see p. 348 in [34]), which is called the time-constant. For the proposed 1R system, we have Q cells to adapt sequentially. To ensure that the steady state can be achieved closely, we let the adaptation time be four time-constants for each cell. Therefore, the overall adaptation time for the 1R system, denoted as N_1, is then $4Q\lceil 1/\mu_c \rceil$. Let the step size for the adaptive filter in the 1R system and that in the HRAF be the same (i.e., $\mu_c = \mu_H \triangleq \mu$). For multirate systems described in Section 3, we further let $\mu_L = \mu/D$ and $\mu_M = \mu/D_M$. In this way, the variances of these adaptive filter taps are the same (see Eqs. (7) and (29)).

4.2.1. 2R scheme

An acquisition error may occur due to $\hat{\alpha} \neq \alpha$, $\hat{\Delta} \neq \Delta$, or both. When the phase feedback to PTF is not correct, i.e., $\hat{\Delta} \neq \Delta$, the peak magnitude of $w_{L,\alpha}(m)$ will be reduced, and the overall acquisition performance will be affected. If we assume that there are no decision errors, the probability of acquisition error for the time instant n, denoted as $P_e(n)$, can be written as

$$P_e(n) = 1 - P_{L,c}(m)P_{H,c}(n), \tag{41}$$

$$P_{L,c}(m) = P(w_{L,c}(m) \geqslant w_{L,j}(m)), \quad c \neq j, \ \ \{c,j\} \in \{0,1,\ldots,M_p\}, \tag{42}$$

$$P_{H,c}(n) = P(w_{H,c}(n) \geqslant w_{H,j}(n)), \quad c \neq j, \ \ \{c,j\} \in \{-D/2,\ldots,0,\ldots,D/2\}, \tag{43}$$

where $P_{L,c}(m)$ and $P_{H,c}(n)$ denote the correct acquisition probabilities of the LRAF and HRAF, respectively. Also, $w_{L,c}(m)$ and $w_{H,c}(n)$ denote the taps whose tap-indices correspond to the actual code delay.

Using the transient analysis of LMS algorithms in [33], we have the mean weight vector of the LRAF as

$$E\{\mathbf{w}_L(m)\} = [\mathbf{I} - (\mathbf{I} - \mu_L\mathbf{R}_L)^m]\mathbf{w}_{L,o}, \tag{44}$$

and the (M_p+1)-by-(M_p+1) covariance matrix as

$$\mathbf{C}_L(m) = \frac{\mu_L D\sigma_v^2}{2}[\mathbf{I} - (\mathbf{I} - 2\mu_L\mathbf{R}_L)^m]. \tag{45}$$

Since $\mathbf{R}_L = D\mathbf{I}$, we can let $\mathbf{C}_L(m) = \sigma^2_{w_L}(m)\mathbf{I}$ where $\sigma^2_{w_L}(m)$ is an equivalent variance that can be derived from (45). Here, $\mathbf{w}_L(m)$ and $\mathbf{w}_H(n)$ are assumed to be Gaussian distributed. Similarly, we can have the mean weight vector and the covariance matrix of $\mathbf{w}_H(n)$ as

$$E\{\mathbf{w}_H(n)\} = [\mathbf{I} - (\mathbf{I} - \mu_H\mathbf{R}_H)^n]\mathbf{w}_{H,o}, \tag{46}$$

and

$$\mathbf{C}_H(n) = \frac{\mu_H\sigma_v^2}{2}[\mathbf{I} - (\mathbf{I} - 2\mu_H\mathbf{R}_H)^n]. \tag{47}$$

Since $\mathbf{R}_H = \mathbf{I}$, we can let $\mathbf{C}_H(n) = \sigma^2_{w_H}(n)\mathbf{I}$. Similarly, $\sigma^2_{w_H}(n)$ is an equivalent variance that can be derived from (47). From Eqs. (45) and (47), we find that tap-weights are independent and identically distributed. As mentioned, both the HRAF and LRAF are run for N chips. For notational simplicity, we let A_L as the peak in $E\{\mathbf{w}_L(\lfloor N/D \rfloor)\}$, $\sigma_L^2 = \sigma^2_{w_L}(\lfloor N/D \rfloor)$, $P_L = P_{L,c}(\lfloor N/D \rfloor)$, A_H as the peak in $E\{\mathbf{w}_H(N)\}$, $\sigma_H^2 = \sigma^2_{w_H}(N)$, $P_H = P_{H,c}(N)$, and $P_e = P_e(N)$. The probabilities in Eqs. (42) and (43) at $n = N$ turn out to be

$$P_L = \frac{1}{\sqrt{2\pi\sigma_L^2}}\int_{-\infty}^{\infty}\left[1 - Q\left(\frac{w}{\sigma_L}\right)\right]^{M_p}\exp\left(-\frac{(w-A_L)^2}{2\sigma_L^2}\right)\mathrm{d}w, \tag{48}$$

$$P_H = \frac{1}{\sqrt{2\pi\sigma_H^2}}\int_{-\infty}^{\infty}\left[1 - Q\left(\frac{w}{\sigma_H}\right)\right]^{D}\exp\left(-\frac{(w-A_H)^2}{2\sigma_H^2}\right)\mathrm{d}w. \tag{49}$$

Finally, we obtain

$$P_e = 1 - P_L P_H. \tag{50}$$

As mentioned in Section 3, incorrect decisions can occur and the error propagation between the HRAF and LRAF will lower the peak amplitudes of final tap-weights. Thus, the results in Eqs. (48)–(50) may be too optimistic. However, the exact analysis of the error propagation effect turns out to be very difficult, if not impossible. In what follows, we propose a simple approximation method to overcome the problem. We first assume that the error propagation affects the mean of a tap-weight much more serious than the variance. As a result, we only consider the variation of mean weight vectors. For an adaptation period, a decision error can occur in any instant and the error sequence can have many patterns. For simplicity, we only investigate those affecting performance most. Consider the LRAF. It is simple to see that if there are κ decision errors during the adaptation period (i.e., between $m = 0$ and $\lfloor N/D \rfloor$), the error pattern corresponding to the worst performance will be the one when all errors occur between $m = \lfloor N/D \rfloor - \kappa + 1$ and $\lfloor N/D \rfloor$. In other words, once a decision error occurs, the error will continue to the end of the adaptation period. This will make the peak weight value of the LRAF decrease from $m = \lfloor N/D \rfloor - \kappa + 1$ monotonically. We then use this pattern to represent all possible error patterns having κ decision errors. From (44), we have $A_L = 1 - (1 - \mu_L D)^{\lfloor N/D \rfloor}$. Taking the decision

errors into account, we may then rewrite A_L as

$$A_L(\kappa) = [1-(1-\mu_L D)^{\lfloor N/D \rfloor - \kappa}] \exp\left(-\frac{\kappa}{\eta_L}\right), \quad (51)$$

where $\eta_L^{-1} = \mu_L \lambda_L$ and $\lambda_L = D$ is the eigenvalue of $\mathbf{R}_L$ [34]. We may treat κ as a random variable with a binomial distribution as

$$p(\kappa) = \binom{\lfloor N/D \rfloor}{\kappa} (1-P_L)^{\kappa} P_L^{\lfloor N/D \rfloor - \kappa}, \quad (52)$$

where P_L is the correct probability in (48). We then use Eqs. (51) and (52) to calculate the mean value of $A_L(\kappa)$, denoted as $\bar{A}_L$. It is given by

$$\bar{A}_L = \sum_{\kappa=0}^{\lfloor N/D \rfloor} A_L(\kappa) p(\kappa). \quad (53)$$

Then, the probability of correct acquisition for the LRAF, denoted as $\bar{P}_L$, can be obtained by substituting $\bar{A}_L$ into (48). Similarly, we can use the same procedure to obtain the probability of correct acquisition for the HRAF, $\bar{P}_H$. Finally, the probability of acquisition error for a 2R system, denoted as P_E, is obtained by

$$P_E = 1 - \bar{P}_L \bar{P}_H. \quad (54)$$

It is worth mentioning that P_L and P_H are the correct acquisition probabilities without decision errors. Thus, these values essentially correspond to two upper bounds of the correct acquisition probabilities. Using these values in the calculation of $p(\kappa)$ (as that in (52)) will underestimate the acquisition error probability. On the other hand, we only take the worst decision error patterns into consideration and this will overestimate the acquisition error probability. Thus, (54) is a result corresponding a compromise of these two extreme cases.

4.2.2. 3R scheme

Using the similar idea, we can have the probability of acquisition error for the decision-error-free case as

$$P_e(n) = 1 - P_{L,c}(m) P_{M,c}(s) P_{H,c}(n), \quad (55)$$

$$P_{L,c}(m) = P(w_{L,c}(m) \geqslant w_{Lj}(m)), \quad c \neq j, \ \{c,j\} \in \{0,1,\ldots,M_p\}, \quad (56)$$

$$P_{M,c}(s) = P(w_{M,c}(s) \geqslant w_{Mj}(s)), \quad c \neq j, \ \{c,j\} \in \{-D/(2D_M),\ldots,0,\ldots,D/(2D_M)\}, \quad (57)$$

$$P_{H,c}(n) = P(w_{H,c}(n) \geqslant w_{Hj}(n)), \quad c \neq j, \ \{c,j\} \in \{-D_M/2,\ldots,0,\ldots,D_M/2\}, \quad (58)$$

where $P_{L,c}(m)$, $P_{M,c}(s)$, and $P_{H,c}(n)$ are the correct acquisition probabilities of the LRU, MRU, and HRU, respectively; $w_{L,c}(m)$, $w_{M,c}(s)$, $w_{H,c}(n)$ denote the taps whose tap-indices correspond to the actual code delay. Note that $s = \lfloor n/D_M \rfloor$. Let $P_L = P_{L,c}(\lfloor N/D \rfloor)$, $P_M = P_{M,c}(\lfloor N/D_M \rfloor)$, $P_H = P_{H,c}(N)$, and $P_e = P_e(N)$. Then P_L can be calculated as that in (48), while P_M and P_H are given by

$$P_M = \frac{1}{\sqrt{2\pi\sigma_M^2}} \int_{-\infty}^{\infty} \left[1 - Q\left(\frac{w}{\sigma_M}\right)\right]^{D/D_M} \exp\left(-\frac{(w-A_M)^2}{2\sigma_M^2}\right) dw,$$
$$P_H = \frac{1}{\sqrt{2\pi\sigma_H^2}} \int_{-\infty}^{\infty} \left[1 - Q\left(\frac{w}{\sigma_H}\right)\right]^{D_M} \exp\left(-\frac{(w-A_H)^2}{2\sigma_H^2}\right) dw, \quad (59)$$

where A_M and σ_M^2 can be obtained as that described in Eqs. (44) and (45). Then, we have $P_e = 1 - P_L P_M P_H$. Again, P_e does not consider the decision error propagation effect. We can follow the same notation definitions and procedures outlined in the previous subsection to obtain $\{\bar{P}_L, \bar{P}_M, \bar{P}_H\}$. Finally, we have the probability of acquisition error for the 3R system as

$$P_E = 1 - \bar{P}_L \bar{P}_M \bar{P}_H. \quad (60)$$

4.3. Mean acquisition time

Mean acquisition time analysis is generally derived with a Markov chain model [36]. Since our multirate systems is different from the MF with serial search, the commonly used model [10] cannot be applied here. Fig. 4 shows the model derived for our systems. As the figure shows, the system iterates for N chips to obtain $\hat{\tau}$ and the probability of acquisition error is P_E. If the acquisition fails, it will wait for a period of time T_p (chips) before the system re-starts the acquisition. Here, T_p is generally referred to as the penalty time [32]. For our schemes, $\hat{\tau}$ is constructed from $\{\hat{\alpha}, \hat{\Delta}\}$ or $\{\hat{\alpha}, \hat{\beta}, \hat{\delta}\}$ at $n = N$. If $\hat{\tau} \neq \tau$, the receiver will re-initialize acquisition after a time interval of T_p chips. We can have the transfer function of the Markov chain model in Fig. 4 as [27,36]

$$H(z) = \frac{(1-P_E) z^N}{1 - P_E z^{T_p+N}}, \quad (61)$$

where z is a delay operator and P_E is the probability of acquisition error formulated above. The mean acquisition

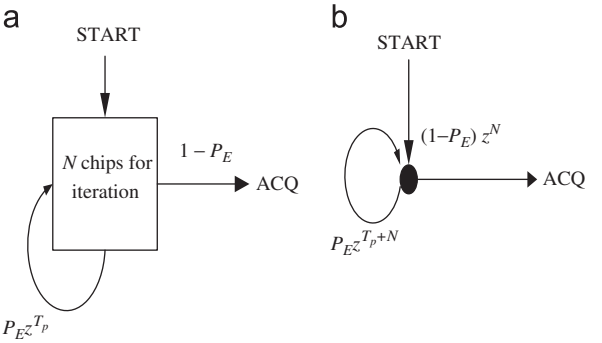

Fig. 4. Markov chain model for multirate code acquisition schemes. The right hand side figure illustrates an equivalent model, where z is a delay operator, P_E the probability of acquisition error, T_p penalty time, and ACQ the correct acquisition state.

time can then be easily found as

$$T_{acq} \triangleq \frac{\mathrm{d}}{\mathrm{d}z} H(z)|_{z=1} \tag{62}$$

$$= N + \frac{(T_p + N)P_E}{(1 - P_E)}. \tag{63}$$

Note that the unit of T_{acq} is chip.

5. Simulation results

In this section, we conduct computer simulations to demonstrate the effectiveness of the proposed algorithms. First, we investigate the computational complexity issue. Using Eqs. (38) and (40), we can evaluate the computational complexity requirement per chip versus D for 1R, 2R, and 3R schemes. We list the results in Tables 1–3 for $D = 4$, 8, and 16, respectively. The numbers inside the parentheses in these tables indicate the values of D_M used for the 3R system. Also, the last two rows of the tables give the complexity ratio defined as C_2/C_1 and C_3/C_1, respectively. From these tables, we can have several observations. Firstly, the larger the processing gain, the higher efficiency the multirate system can achieve. Secondly, the 3R system is always more efficient than the 2R system. Lastly, there exists an optimum D for a given processing gain L. For example, when $L = 1024$ and $D = 8$, the computational complexity of the 2R system is about 20% of the 1R system. For the same processing gain with $D = 16$, the complexity of the 3R system is only about 16% of the 1R system. These outcomes state that the multirate system can be much more efficient than the 1R system for large L.

Table 1
Computational complexity comparison for $D = 4$.

L	128	256	512	1024
C_1	64	128	256	512
C_2	26.50	42.50	74.50	138.50
C_3	25.5 (2)	41.5 (2)	73.5 (2)	137.5 (2)
C_2/C_1	0.414	0.332	0.291	0.271
C_3/C_1	0.398	0.324	0.287	0.269

Table 2
Computational complexity comparison for $D = 8$.

L	128	256	512	1024
C_1	32	64	128	256
C_2	22.25	26.25	34.25	50.25
C_3	14.25 (3)	18.25 (3)	26.25 (3)	42.25 (3)
C_2/C_1	0.695	0.410	0.268	0.196
C_3/C_1	0.445	0.285	0.205	0.165

Table 3
Computational complexity comparison for $D = 16$.

L	128	256	512	1024
C_1	16	32	64	128
C_2	35.125	36.125	38.125	42.125
C_3	13.125 (3)	14.125 (3)	16.125 (3)	20.125 (3)
C_2/C_1	2.195	1.129	0.596	0.329
C_3/C_1	0.821	0.441	0.252	0.157

We set signal-to-interference-plus-noise ratio (SINR_c), which is defined $1/\sigma_v^2$, as -13 dB (about 20 users with equal power). Also, $L = 128$, $D = 8$, $D_M = 4$, $\mu = \mu_H = \mu_L D = \mu_M D/2$, and $N = 4D\lceil 1/\mu \rceil$. To show how the proposed scheme works, we let $\tau = 51$ and use a 3R system with above parameter setting to conduct simulations (100 trials). Fig. 5 shows the averaged peak-weight positions associated with the LRAF, the MRAF, and the HRAF. As we can see, $\hat{\alpha} = 7, \hat{\beta} = -1$, and $\hat{\gamma} = -1$. Thus, the code delay can be estimated as $\hat{\tau} = \hat{\alpha}D + \hat{\beta}D_M + \hat{\gamma} = 51$, which is equal to the actual delay. We then compare the probabilities of acquisition error for 1R, 2R, and 3R systems. The code delay, τ, here is uniformly and randomly selected from $[0, L)$. We conduct 10^4 independent trials and show the results in Fig. 6. Also shown in the figure is the theoretical results derived in Section 4. Experimental results in Fig. 6 indicate that the performance of multirate systems are slightly better than that of the 1R system. Theoretical predictions for all systems are accurate particularly when the step size is large. For the 1R system, the deviation between experimental and theoretical values is smaller than that in 2R and 3R systems. This is not surprising, since the 1R system does not have the error propagation problem.

As mentioned, an important acquisition performance measure is the mean acquisition time. To derive the mean acquisition time, T_{acq}, we first set $T_p = 1.28 \times 10^4$ chips (100 bits) and substitute the experimental acquisition error probabilities obtained from Fig. 6 into (63). Fig. 7 shows the mean acquisition time for all systems. The lower bound in Fig. 7 corresponds to the case that no acquisition errors occur. In this case, $T_{acq} = N = 4D\lceil 1/\mu \rceil$ and this can serve as a performance bound for comparison. As we can see, ini-tially the mean acquisition time decreases when the step size increases. When the step size is larger than $\mu = 5 \times 10^{-3}$, the mean acquisition time starts to increase. For the setting here, the optimal step size is around $\mu = 5 \times 10^{-3}$. In this case, T_{acq} for the 1R system is about 7500 chips, that for the 2R system is about 7150 chips, and that for the 3R system is about 7250 chips. We also examine the probability of acquisition error for various SINR_c. Fig. 8 shows the experimental results. Here, we let $\mu = 5 \times 10^{-3}$, $L = 128$, $D = 8$, $D_M = 4$, and $N = 4D\lceil 1/\mu \rceil$. We find that all systems have similar performance. Also, the higher the SINR_c, the better performance we can have. The 2R system behaves slightly better than the others. Fig. 9 shows the corresponding mean acquisition time. In terms of the mean acquisition time, we have the same conclusion that all systems have similar performance.

For all simulations shown above, we have fixed $N = 4D\lceil 1/\mu \rceil$ for the systems. In terms of mean acquisition time, this choice may not be optimal. Fig. 10 shows the mean acquisition time for various N (SINR_c is -13 dB). As we can see, there are optimum N's for multirate systems. For $\mu = 5 \times 10^{-3}$, we find that the mean acquisition time of the 3R system increases quicker than that of the 2R system when N is smaller than the optimum value. This is because the performance of low-rate units depends on N

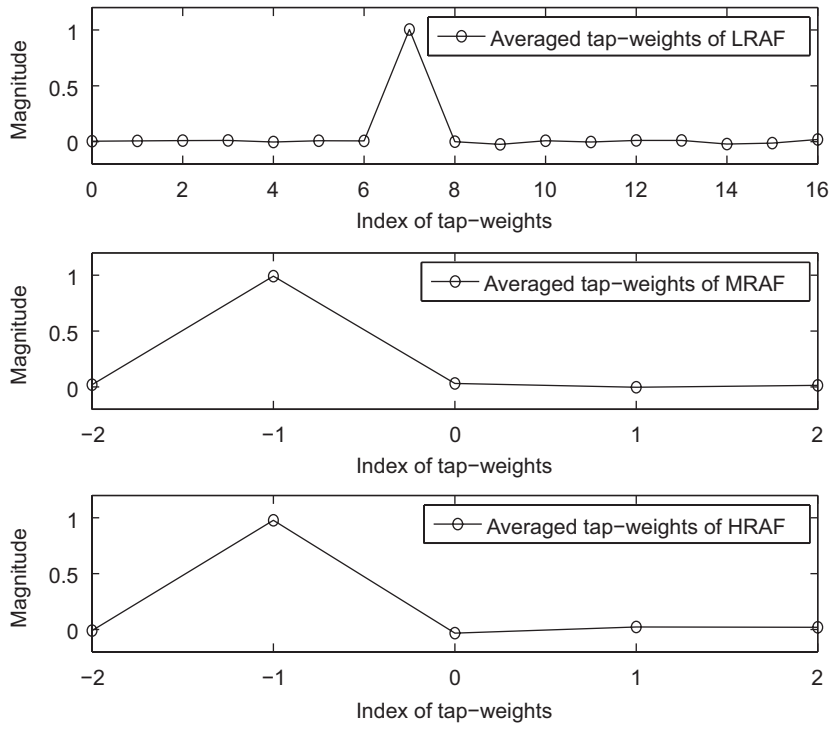

Fig. 5. Averaged tap-weights for LRAF, MRAF, and HRAF for 3R systems. ($L = 128$, $D = 8$, $D_M = 4$, $\tau = 51$, $\mu = 4 \times 10^{-3}$, $\mathrm{SINR}_c = -13$ dB, and 100 trials.)

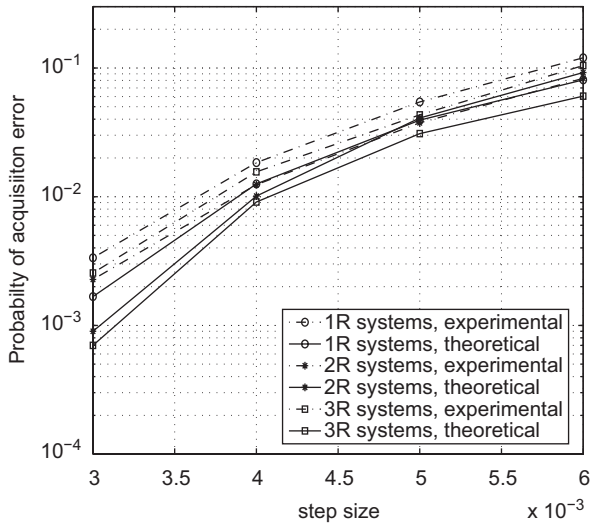

Fig. 6. Experimental and theoretical P_E ((9), Eqs. (54) and (60)) versus step size μ ($D = 8$, $D_M = 4$, $L = 128$, and $\mathrm{SINR}_c = -13$ dB).

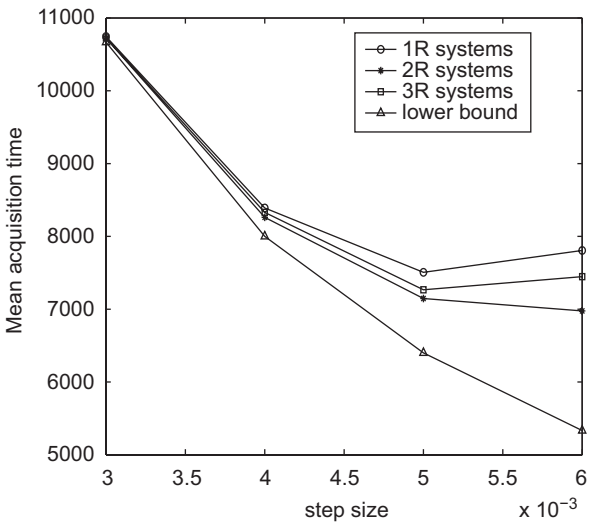

Fig. 7. Experimental mean acquisition time T_{acq} versus step size μ ($T_p = 1.28 \times 10^4$, $D = 8$, $D_M = 4$, and $\mathrm{SINR}_c = -13$ dB).

more strongly. When N is larger than the optimum value, the mean acquisition times of both systems approach the lower bounds. We can observe the same behaviors when $\mu = 3 \times 10^{-3}$. From the figure, we also find that the optimal N is about 2 and 2.5 time-constants for $\mu = 3 \times 10^{-3}$ and 5×10^{-3}, respectively. In these cases, $T_{acq} = 6 \times 10^3$ chips (47 bits) for both step sizes.

6. Conclusions

The performance of conventional code acquisition in a CDMA system degrades greatly when MAI presents. The adaptive filtering approach proposed recently has been proven to be MAI-resistant. In this paper, we propose a multirate adaptive code acquisition scheme that can

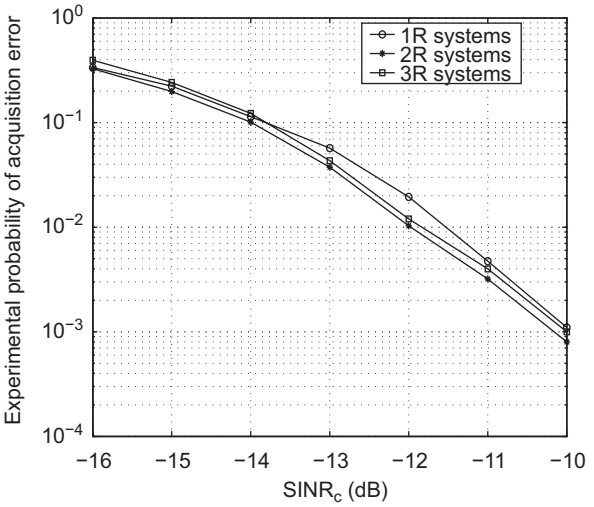

Fig. 8. Experimental P_E versus SINR$_c$ ($\mu = 5 \times 10^{-3}$).

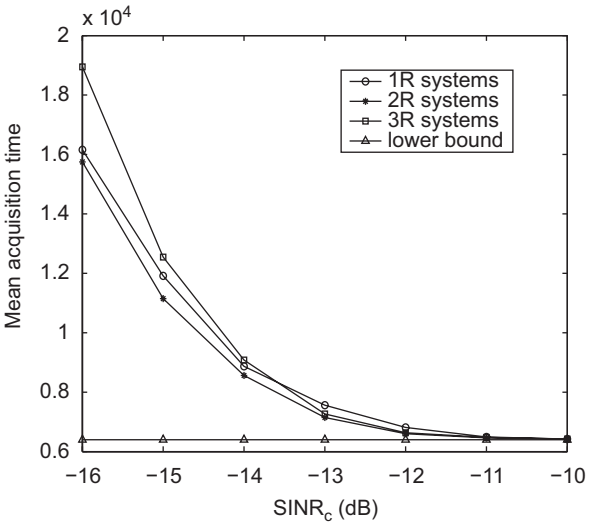

Fig. 9. Experimental mean acquisition time T_{acq} versus SINR$_c$ ($\mu = 5 \times 10^{-3}$).

significantly reduce the required computational complexity. We have specifically studied the 2R and 3R systems and theoretically analyzed their performance; this includes the filter convergence properties, acquisition error rate, and mean acquisition time. Experimental results show that while the proposed schemes can perform similarly with the conventional adaptive acquisition, the computational complexity is much lower. The proposed scheme is specially suitable for CDMA systems operating in large propagation delay environments. With proper choice of D or D_M, the multirate code acquisition scheme can achieve an efficient compromise between the mean acquisition time and computational complexity. The proposed scheme can also be used in a carrier-phase unsynchronized system. In this circumstance, we have to take the inphase as well as quadrature components of tap-weights into account. If the

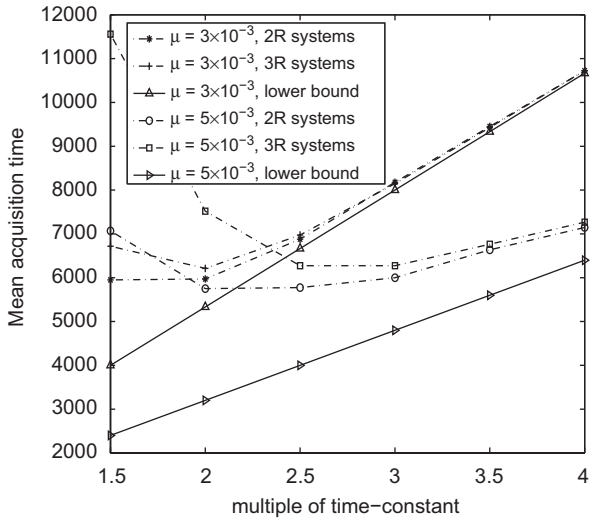

Fig. 10. Experimental mean acquisition time T_{acq} versus N (expressed as a multiple of time-constant) and step size μ.

code delay has a fractional part, the optimum tap-weights will have two peaks and this will enlarge the MMSE, which in turn affects the acquisition performance. To mitigate this problem, we can oversample the receive signal and conduct a sub-chip level acquisition. In this paper, we only consider the scenario of the AWGN channel. It is straightforward to extend the use of the proposed scheme to multipath channels. In this case, the HRAF will acquire the signal from the strongest path. The performance analysis can then serve as a potential topic for further research.

Acknowledgement

The authors would like to thank the valuable comments from Ren-Jr Chen who is working in the Info. & Comm. Research Lab., ITRI, Taiwan.

Appendix A

In this section, the optimal tap-weights of a LRAF with different Δ will be derived. With the results, the steady-state MSE of a LRAF can be evaluated. To simplify the notation, we let

$$\rho = \frac{|\Delta|}{D}. \tag{A.1}$$

A.1. The case of $\Delta \geqslant 0$

Consider the case where $\Delta \geqslant 0$ first. The element $x_L(m-\varepsilon)$, $\varepsilon \in \{0, 1, \ldots, M_p\}$ in (18) can be rewritten as

$$\begin{aligned} x_L(m-\varepsilon) &= \sum_{j=0}^{D-1} x((m-\varepsilon)D - j) \\ &= \sum_{j=0}^{\Delta-1} x((m-\varepsilon)D - j) + \sum_{j=\Delta}^{D-1} x((m-\varepsilon)D - j) \end{aligned}$$

$$= \sum_{j=0}^{\Delta-1} x((m-\varepsilon)D-j) + \sum_{j=0}^{D-\Delta-1} x((m-\varepsilon)D-\Delta-j)$$
$$= \sqrt{D\rho}\left\{\frac{1}{\sqrt{D\rho}}\sum_{j=0}^{\Delta-1} x((m-\varepsilon)D-j)\right\} + \sqrt{D(1-\rho)}\left\{\frac{1}{\sqrt{D(1-\rho)}} \sum_{j=0}^{D-\Delta-1} x((m-\varepsilon)D-\Delta-j)\right\}. \quad (A.2)$$

Let

$$\theta(m) = \frac{1}{\sqrt{D\rho}}\sum_{j=0}^{\Delta-1} x(mD-j), \quad (A.3)$$

$$\phi(m) = \frac{1}{\sqrt{D(1-\rho)}}\sum_{j=0}^{D-\Delta-1} x(mD-\Delta-j), \quad (A.4)$$

$\mathbf{\Theta}(m) = [\theta(m), \theta(m-1), \ldots, \theta(m-M_p)]^{\mathrm{T}}$, and $\mathbf{\Phi}(m) = [\phi(m), \phi(m-1), \ldots, \phi(m-M_p)]^{\mathrm{T}}$. Thus, (A.2) can be written as

$$x_L(m-\varepsilon) = \sqrt{D\rho}\theta(m-\varepsilon) + \sqrt{D(1-\rho)}\phi(m-\varepsilon), \quad \varepsilon \in \{0,1,\ldots,M_p\}, \quad (A.5)$$

and (18) as

$$\mathbf{x}_L(m) = \sqrt{D\rho}\mathbf{\Theta}(m) + \sqrt{D(1-\rho)}\mathbf{\Phi}(m). \quad (A.6)$$

Note that $\theta(m)$, $\phi(m)$ and $v_L(m)$ are zero mean, mutually uncorrelated, and

$$E\{\theta(m)\theta(m-\varepsilon)\} = \delta(\varepsilon),$$
$$E\{\phi(m)\phi(m-\varepsilon)\} = \delta(\varepsilon),$$
$$E\{v_L(m)v_L(m-\varepsilon)\} = D\sigma_v^2\delta(\varepsilon), \quad (A.7)$$

where $\delta(\cdot)$ denotes a Kronecker Dirac delta function. Using Eqs. (A.3) and (A.4), we can also express (15) as

$$r_L(m) = \sum_{j=0}^{D-1} x((m-\alpha)D-\Delta-j) + v_L(m)$$
$$= \sum_{j=0}^{D-\Delta-1} x((m-\alpha)D-\Delta-j) + \sum_{j=D-\Delta}^{D-1} x((m-\alpha)D-\Delta-j) + v_L(m)$$
$$= \sum_{j=0}^{D-\Delta-1} x((m-\alpha)D-\Delta-j) + \sum_{j=0}^{\Delta-1} x((m-\alpha-1)D-j) + v_L(m)$$
$$= \sqrt{D(1-\rho)}\phi(m-\alpha) + \sqrt{D\rho}\theta(m-\alpha-1) + v_L(m). \quad (A.8)$$

Let the tap-weights of the LRAF be $\mathbf{w}_L(m) = [w_{L,0}(m), w_{L,1}(m), \ldots, w_{L,M_p}(m)]^{\mathrm{T}}$. Also, let the corresponding optimal solution be $\mathbf{w}_{L,o}$. Using the corresponding Wiener equations, we can have

$$\mathbf{w}_{L,o} = \mathbf{R}_L^{-1}\mathbf{p}_L, \quad (A.9)$$

where $\mathbf{p}_L \triangleq E\{\mathbf{x}_L(m)r_L(m)\}$ and $\mathbf{R}_L \triangleq E\{\mathbf{x}_L(m)\mathbf{x}_L^{\mathrm{T}}(m)\}$. From Eqs. (A.6) and (A.7), it is simple to derive

$$\mathbf{R}_L = D\mathbf{I}. \quad (A.10)$$

Using Eqs. (A.6) and (A.8), we can find the cross-correlation between $r_L(m)$ and $\mathbf{x}_L(m)$ as

$$\mathbf{p}_L = \left[\underbrace{0,\ldots,0}_{\alpha}, D-\Delta, \Delta, 0, \ldots, 0\right]^{\mathrm{T}} \quad (A.11)$$

From (A.9), we obtain

$$w_{L,o,\varepsilon} = \begin{cases} 1-\rho, & \varepsilon = \alpha, \\ \rho, & \varepsilon = \alpha+1, \\ 0 & \text{otherwise}, \end{cases} \quad \varepsilon \in \{0,1,\ldots,M_p\}, \quad (A.12)$$

where $w_{L,o,\varepsilon}$ is the εth element of $\mathbf{w}_{L,o}$. Let the MSE that the Wiener filter minimizes be $J_L(m)$. Then,

$$J_L(m) = E\{[r_L(m) - \mathbf{w}_L^{\mathrm{T}}(m)\mathbf{x}_L(m)]^2\}$$
$$= E\{r_L^2(m)\} - 2\mathbf{w}_L^{\mathrm{T}}(m)\mathbf{p}_L + \mathbf{w}_L^{\mathrm{T}}(m)\mathbf{R}_L\mathbf{w}_L(m), \quad (A.13)$$

where $E\{r_L^2(m)\} = DE\{r^2(n)\} = D(\sigma_v^2+1)$. Replacing $\mathbf{w}_L(m)$ with $\mathbf{w}_{L,o}$, we can obtain the corresponding MMSE, $J_{L,min}$, as

$$J_{L,min} = DE\{r^2(n)\} - D[(1-\rho)^2 + \rho^2]$$
$$= D[\sigma_v^2 + 2\rho(1-\rho)]. \quad (A.14)$$

From (A.14), we can see that a nonzero ρ will produce an extra term in the MMSE. We now proceed to find the MSE yielded by the LMS algorithm. Using Eqs. (A.6) and (A.12), we derive

$$\mathbf{x}_L^{\mathrm{T}}(m)\mathbf{w}_{L,o} = (1-\rho)\{\sqrt{D\rho}\theta(m-\alpha) + \sqrt{D(1-\rho)}\phi(m-\alpha)\} + \rho\{\sqrt{D\rho}\theta(m-\alpha-1) + \sqrt{D(1-\rho)}\phi(m-\alpha-1)\} \quad (A.15)$$
$$= \sqrt{D\rho}\theta(m-\alpha) + \sqrt{D(1-\rho)}\phi(m-\alpha) - \rho\sqrt{D\rho}\theta(m-\alpha) - \rho\sqrt{D(1-\rho)}\phi(m-\alpha) + \rho\sqrt{D\rho}\theta(m-\alpha-1) + \rho\sqrt{D(1-\rho)}\phi(m-\alpha-1). \quad (A.16)$$

Substituting (A.8) into (A.16), we obtain

$$\mathbf{x}_L^{\mathrm{T}}(m)\mathbf{w}_{L,o} = r_L(m) - v_L(m) + (1-\rho)\sqrt{D\rho} \times\{\theta(m-\alpha) - \theta(m-\alpha-1)\} - \rho\sqrt{D(1-\rho)}\{\phi(m-\alpha) - \phi(m-\alpha-1)\}. \quad (A.17)$$

Rewriting (A.17), we have

$$r_L(m) = \mathbf{x}_L^{\mathrm{T}}(m)\mathbf{w}_{L,o} + v_L(m) \underbrace{-(1-\rho)\sqrt{D\rho}[\theta(m-\alpha) - \theta(m-\alpha-1)] + \rho\sqrt{D(1-\rho)}[\phi(m-\alpha) - \phi(m-\alpha-1)]}_{\triangleq \xi(m)}, \quad (A.18)$$

where $\xi(m)$ is zero mean and its variance is $\sigma_\xi^2 = 2D\rho(1-\rho)$. The LMS tap-weight update equation for the LRAF is given by

$$\mathbf{w}_L(m) = \mathbf{w}_L(m-1) + \mu_L \mathbf{x}_L(m)[r_L(m) - \mathbf{x}_L^{\mathrm{T}}(m)\mathbf{w}_L(m-1)], \tag{A.19}$$

where μ_L is the step size. Substituting (A.18) into (A.19), we have

$$\mathbf{w}_L(m) = \mathbf{w}_L(m-1) + \mu_L \mathbf{x}_L(m)[\mathbf{x}_L^{\mathrm{T}}(m)\mathbf{w}_{L,o} + v_L(m) + \xi(m) - \mathbf{x}_L^{\mathrm{T}}(m)\mathbf{w}_L(m-1)]. \tag{A.20}$$

Subtracting $\mathbf{w}_{L,o}$ on both sides of (A.20) and letting $\Delta\mathbf{w}_L(m) = \mathbf{w}_L(m) - \mathbf{w}_{L,o}$, we can rewrite (A.20) as

$$\begin{aligned}\Delta\mathbf{w}_L(m) &= \Delta\mathbf{w}_L(m-1) - \mu_L \mathbf{x}_L(m)\mathbf{x}_L^{\mathrm{T}}(m)\Delta\mathbf{w}_L(m-1) + \mu_L \mathbf{x}_L(m)v_L(m) + \mu_L \mathbf{x}_L(m)\xi(m)\\ &= [\mathbf{I} - \mu_L \mathbf{x}_L(m)\mathbf{x}_L^{\mathrm{T}}(m)]\Delta\mathbf{w}_L(m-1) + \mu_L \mathbf{x}_L(m)v_L(m) + \mu_L \mathbf{x}_L(m)\xi(m).\end{aligned} \tag{A.21}$$

Let $\mathbf{Q}(m) = E\{\Delta\mathbf{w}_L(m)\Delta\mathbf{w}_L^{\mathrm{T}}(m)\}$. Then,

$$\begin{aligned}\mathbf{Q}(m) = E\{&[\mathbf{I} - \mu_L \mathbf{x}_L(m)\mathbf{x}_L^{\mathrm{T}}(m)]\Delta\mathbf{w}_L(m-1) \times \Delta\mathbf{w}_L^{\mathrm{T}}(m-1)[\mathbf{I} - \mu_L \mathbf{x}_L(m)\mathbf{x}_L^{\mathrm{T}}(m)]^{\mathrm{T}}\}\\ &+ \mu_L^2 E\{v_L^2(m)\mathbf{x}_L(m)\mathbf{x}_L^{\mathrm{T}}(m)\}\\ &+ \mu_L^2 E\{\xi^2(m)\mathbf{x}_L(m)\mathbf{x}_L^{\mathrm{T}}(m)\}.\end{aligned} \tag{A.22}$$

Eq. (A.22) can be written as

$$\mathbf{Q}(m) = (\mathbf{I} - \mu_L \mathbf{R}_L)\mathbf{Q}(m-1)(\mathbf{I} - \mu_L \mathbf{R}_L) + \mu_L^2 D\sigma_v^2 \mathbf{R}_L + \mu_L^2 \sigma_\xi^2 \mathbf{R}_L. \tag{A.23}$$

Note that in (A.23) we implicitly assume that $\xi^2(m)$ and $\mathbf{x}_L(m)\mathbf{x}_L^{\mathrm{T}}(m)$ are uncorrelated. The εth entry on the main diagonal of $\mathbf{Q}(m)$ is

$$\mathbf{Q}_{\varepsilon,\varepsilon}(m) = (1 - \mu_L D)^2 \mathbf{Q}_{\varepsilon,\varepsilon}(m-1) + \mu_L^2 D^2 \sigma_v^2 + \mu_L^2 D\sigma_\xi^2. \tag{A.24}$$

When $m \longrightarrow \infty$, we have the asymptotic result as

$$\begin{aligned}\mathbf{Q}_{\varepsilon,\varepsilon}(m) &\approx \frac{\mu_L}{2}(D\sigma_v^2 + \sigma_\xi^2)\\ &= \frac{\mu_L D}{2}[\sigma_v^2 + 2\rho(1-\rho)] \quad \varepsilon \in \{0, 1, \ldots, M_p\}.\end{aligned} \tag{A.25}$$

Using Eqs. (A.14) and (A.25), we can have the MSE for the LMS algorithm in steady-state [34] as

$$\begin{aligned}J_L(\infty) &= J_{L,min} + \frac{(M_p+1)\mu_L D}{2}[\sigma_v^2 + 2\rho(1-\rho)]\\ &= \left[1 + \frac{(M_p+1)\mu_L}{2}\right]J_{L,min}.\end{aligned} \tag{A.26}$$

A.2. The case of $\Delta < 0$

Next, let us consider the case where $\Delta < 0$. We define a new set of $\theta(m)$ and $\phi(m)$ as

$$\theta(m) \triangleq \frac{1}{\sqrt{D(1-\rho)}} \sum_{j=0}^{D-|\Delta|-1} x(mD - j), \tag{A.27}$$

$$\phi(m) \triangleq \frac{1}{\sqrt{D\rho}} \sum_{j=0}^{|\Delta|-1} x((m-1)D + |\Delta| - j). \tag{A.28}$$

Then, we can have $x_L(m-\varepsilon)$ as

$$x_L(m-\varepsilon) = \sum_{j=0}^{D-1} x((m-\varepsilon)D - j) \tag{A.29}$$

$$= \sum_{j=0}^{D-|\Delta|-1} x((m-\varepsilon)D - j) + \sum_{j=D-|\Delta|}^{D-1} x((m-\varepsilon)D - j) \tag{A.30}$$

$$= \sum_{j=0}^{D-|\Delta|-1} x((m-\varepsilon)D - j) + \sum_{j=0}^{|\Delta|-1} x((m-\varepsilon-1)D + |\Delta| - j) \tag{A.31}$$

$$= \sqrt{D(1-\rho)}\theta(m-\varepsilon) + \sqrt{D\rho}\phi(m-\varepsilon), \tag{A.32}$$

and (15) as

$$r_L(m) = \sum_{j=0}^{D-1} x((m-\alpha)D + |\Delta| - j) + v_L(m) \tag{A.33}$$

$$= \sum_{j=0}^{|\Delta|-1} x((m-\alpha)D + |\Delta| - j) + \sum_{j=|\Delta|}^{D-1} x((m-\alpha)D + |\Delta| - j) + v_L(m) \tag{A.34}$$

$$= \sum_{j=0}^{|\Delta|-1} x((m-\alpha)D + |\Delta| - j) + \sum_{j=0}^{D-|\Delta|-1} x((m-\alpha)D - j) + v_L(m) \tag{A.35}$$

$$= \sqrt{D\rho}\phi(m-\alpha+1) + \sqrt{D(1-\rho)}\theta(m-\alpha) + v_L(m). \tag{A.36}$$

Following the similar procedure for the case that $\Delta \geqslant 0$, we can derive

$$w_{L,o,\varepsilon} = \begin{cases} 1-\rho, & \varepsilon = \alpha,\\ \rho, & \varepsilon = \alpha - 1, \quad \varepsilon \in \{0, 1, \ldots, M_p\},\\ 0 & \text{otherwise,}\end{cases} \tag{A.37}$$

and

$$\begin{aligned}J_L(\infty) &= J_{L,min} + \frac{(M_p+1)\mu_L D}{2}[\sigma_v^2 + 2\rho(1-\rho)]\\ &= \left[1 + \frac{(M_p+1)\mu_L}{2}\right]J_{L,min}.\end{aligned} \tag{A.38}$$

References

[1] A. Polydoros, C.L. Weber, A unified approach to serial search spread-spectrum code acquisition—part II: a matched-filter receiver, IEEE Transactions on Communications 32 (5) (May 1984) 550–560.

[2] R.R. Rick, L.B. Milstein, Parallel acquisition in mobile DS-CDMA systems, IEEE Transactions on Communications 45 (11) (November 1997) 1466–1476.

[3] Yu T. Su, Rapid code acquisition algorithms employing PN matched filters, IEEE Transactions on Communications 36 (6) (June 1988) 724–733.

[4] E. Sourour, S.C. Gupta, Direct-sequence spread-spectrum parallel acquisition in a fading mobile channel, IEEE Transactions on Communications 38 (7) (1990) 992–998.

[5] T.K. Moon, R.T. Short, C.K. Rushforth, Average acquisition time for SSMA channels, in: IEEE Military Communication Conference, 1991, pp. 1042–1046.

[6] G.E. Corazza, V. Degli-Esposti, Acquisition-based capacity estimates for CDMA with imperfect power control, in: IEEE International Symposium on Spread Spectrum Techniques and Applications, vol. 1, July 1994, pp. 325–329.
[7] U. Madhow, M.B. Pursley, Acquisition in direct-sequence spread-spectrum communication networks: an asymptotic analysis, IEEE Transactions on Information Theory 39 (3) (May 1993) 903–912.
[8] R.L. Pickholtz, L.B. Milstein, D.L. Schilling, Spread spectrum for mobile communication, IEEE Transactions on Vehicular Technology 40 (2) (May 1991) 313–322.
[9] A.G. Dabak, Acquisition based capacity of a synchronous direct sequence spread spectrum multiple access technique, in: IEEE International Symposium on Information Theory, 1994, p. 141.
[10] J.K. Holmes, C.C. Chen, Acquisition time performance of PN spread-spectrum systems, IEEE Transactions on Communications 25 (8) (May 1977) 778–783.
[11] H.-C. Hwang, C.-H. Wei, A new blind adaptive interference suppression scheme for acquisition and MMSE demodulation of DS/CDMA signals, IEEE Transactions on Vehicular Technology 49 (3) (May 2000) 875–884.
[12] E.G. Ström, S. Parkvall, S.L. Miller, B.E. Ottersten, Propagation delay estimation in asynchronous direct-sequence code-division multiple access systems, IEEE Transactions on Communications 44 (1) (January 1996) 84–93.
[13] S.E. Bensley, B. Aazhang, Subspace-based channel estimation for code division multiple access communication systems, IEEE Transactions on Communications 44 (8) (August 1996) 1009–1020.
[14] S. Kim, Improved MUSIC algorithm for the code-timing estimation of DS-CDMA multipath-fading channels in multiantenna systems, IEEE Transactions on Vehicular Technology 53 (5) (September 2004) 1354–1369.
[15] P.K.P. Cheung, P.B. Rapajic, CMA-based code acquisition scheme for DS-CDMA systems, IEEE Transactions on Communications 48 (5) (May 2000) 852–862.
[16] R. Wang, H. Li, T. Li, Code-timing estimation for CDMA systems with bandlimited chip waveforms, IEEE Transactions on Wireless Communications 3 (4) (July 2004) 1338–1348.
[17] Y. Ma, K.H. Li, A.C. Kot, G. Ye, A blind code timing estimator and its implementation for DS-CDMA signals in unknown colored noise, IEEE Transactions on Vehicular Technology 51 (6) (November 2002) 1600–1607.
[18] D. Zheng, J. Li, S.L. Miller, E.G. Ström, An efficient code-timing estimator for DS-CDMA signals, IEEE Transactions on Signal Processing 45 (January 1997) 82–89.
[19] M.G. El-Tarhuni, A.U.H. Sheikh, PN code acquisition in CDMA systems using a MMSE adaptive filter, in: IEEE Canadian Conference on Electrical and Computer Engineering, vol. 2, May 1998, pp. 746–749.
[20] M.G. El-Tarhuni, A.U.H. Sheikh, An adaptive filtering PN code acquisition scheme with improved acquisition based capacity in DS/CDMA, in: Ninth IEEE International Symposium on Personal, Indoor and Mobile Radio Communications, vol. 3, September 1998, pp. 1486–1490.
[21] M.G. El-Tarhuni, A.U.H. Sheikh, Adaptive synchronization for spread spectrum systems, in: 46th IEEE Vehicular Technology Conference, vol. 1, 1996, pp. 170–174.
[22] M.G. El-Tarhuni, Application of adaptive filtering to direct-sequence spread-spectrum code synchronization, Ph.D. Thesis proposal, Department of System and Computer Engineering, Carleton university, Canada, January 1996.
[23] T. Yu, J. Kwun, H. Jeon, D. Hong, C. Kang, Noncoherent adaptive code synchronization for DS/CDMA systems, in: IEEE Global Telecommunications Conference, vol. 6, November 2001, pp. 3311–3315.
[24] M.G. El-Tarhuni, A.U.H. Sheikh, Code acquisition of DS/SS signals in fading channels using an LMS adaptive filter, IEEE Communication Letters 2 (4) (April 1998) 85–88.
[25] H.L. Yang, W.R. Wu, Multirate adaptive filtering for DS/CDMA code acquisition, in: IEEE International Symposium on Signal Processing and Information Technology, December 2003, pp. 363–366.
[26] R.F. Smith, S.L. Miller, Acquisition performance of an adaptive receiver for DS-CDMA, IEEE Transactions on Communications 47 (9) (September 1999) 1416–1424.
[27] H.R. Park, B.J. Kang, On the performance of a maximum-likelihood code-acquisition technique for preamble search in a CDMA reverse link, IEEE Transactions on Vehicular Technology 47 (1) (February 1998) 65–74.
[28] TIA/EIA/IS95, Mobile station-base station compatibility standard for dual-mode wideband spread spectrum cellular system: Telecommunications Industry Association, July, 1993.
[29] TIA CDMA. 2000, Wideband cdmaOne radio transmission technology proposal: International Telecommunication Union, Radiocommunication Study Groups, June 1998.
[30] E. Dahlman, et al., WCDMA—the radio interface for future mobile multimedia communications, IEEE Transactions on Vehicular Technology 47 (November 1998) 1105–1118.
[31] P. Taaghol, et al., Satellite UMTS/IMT2000 W-CDMA air interfaces, IEEE Communications Magazine 37 (September 1999) 116–126.
[32] A.J. Viterbi, Principle of Spread Spectrum Communications, Addison-Wesley, New York, 1995.
[33] N.J. Bershad, L.Z. Qu, On the probability density function of the LMS adaptive filter weights, IEEE Transactions on Acoustics, Speech, and Signal Processing 37 (1) (January 1989) 43–56.
[34] S. Haykin, Adaptive Filter Theory, third ed., Prentice-Hall, Englewood Cliffs, NJ, 1996.
[35] J.G. Proakis, Digital Communications, fourth ed., McGraw-Hill, New York, 2000.
[36] J.K. Holmes, Coherent Spread Spectrum Systems, Wiley, New York, 1982.